Protection coordination considering different characteristic curves and a variable limit of the plug setting multiplier

Coordinación de protecciones considerando diferentes curvas características y un límite variable del multiplicador de ajuste

S. D. Saldarriaga-Zuluaga ; J. M. López-Lezama ; N. Muñoz-Galeano

DOI: https://doi.org/10.22517/23447214.24731
Article of scientific and technological research

***Abstract*— This paper presents a methodology for protection coordination in microgrids that considers account non-standard features of directional over-current relays (OCRs). In the proposed approach three decision variables are considered for each relay; namely, the standard characteristic curve (*SCC*), Time Multiplier Setting (*TMS*) and maximum limit of the plug setting multiplier (*PSM*). The proposed mixed integer non-linear programing model is solved by means of a specialized genetic algorithm (GA) implemented in Matlab. Several tests were performed on a modified version of the IEEE-30 bus test system considering on-grid and off-grid operational modes. The results evidenced the robustness and applicability of the proposed approach in real-size microgrids that host distributed generation and exhibit several operational modes or topologies.**

***Index Terms*— Distribution systems, genetic algorithms, microgrids, protection coordination, relés.**

***Resumen*— Este trabajo presenta una metodología para la coordinación de protecciones en microrredes que tiene en cuenta las características no estándar de los relés de sobrecorriente direccionales (OCR). En el enfoque propuesto se consideran tres variables de decisión para cada relé: la curva característica estándar (*SCC*), el ajuste del multiplicador del tiempo (*TMS*) y su respectivo límite máximo (*PSM*). El modelo de programación no lineal entero mixto propuesto se resuelve mediante un algoritmo genético especializado (GA) implementado en Matlab. Se realizaron varias pruebas en una versión modificada del sistema de prueba de bus IEEE-30 considerando los modos de funcionamiento en red y fuera de red. Los resultados evidenciaron la robustez y aplicabilidad del enfoque propuesto en microrredes de tamaño real que albergan generación distribuida y presentan varios modos o topologías de funcionamiento.**

***Palabras claves*— Algoritmos genéticos, coordinación de protecciones, microrredes, relays, sistemas de distribución.**

I. Introduction

MODERN distribution networks must deal with new challenges such as the increasing presence of renewable distributed generation (DG) and a more active role of consumers. In this scenario, protection coordination of distribution networks must be revised since traditional approaches based on unidirectional power flows are no longer applicable. Microgrids play a key role in modern distribution networks since they facilitate the integration of DG. Nonetheless, several technical issues must be discussed for their suitable incorporation; one of them is the protection coordination problem. The fact that microgrids may operate under different topologies render inefficient the conventional paradigm of protection coordination based on fixed short circuit levels and unidirectional power flows. The authors in [1] present a review on issues and approaches for microgrid protection. They indicate that the integration of microgrids in modern distribution networks causes the magnitude of fault currents to change dynamically depending on several factors such as the operation modes of the microgrid, as well as the type and status of DG within the network. Furthermore, conventional protection schemes are usually designed for radial power flows with centralized generation. This makes traditional protection schemes inappropriate for bilateral power flows as in the case of microgrids. In this sense, there is a constant search of new models and methodologies regarding the protection coordination problem of microgrids.

In [2], a hybrid particle swarm optimization (HPSO) approach is proposed for solving the protection coordination of directional overcurrent relays (DOCR) in microgrids. In this case, two operative modes of the network are considered. Furthermore, only two decision variables are considered for each relay: the current setting (taken as a discrete parameter) and the time multiplier setting (*TMS*). The optimization procedure is carried out in two stages. In the first one, a discrete PSO is used to calculate the current setting, while in the second one, linear programming is applied to calculate the *TMS* of each relay. The main limitation of this approach lies on the fact that it only considers two optimization variables per relay. Also, the current setting is considered as a discrete variable instead of as a continuous one. Furthermore, dividing the optimization problem into two different procedures makes the problem more likely to achieve sub-optimal solutions.

In [3], the authors solve the protection coordination and power

This manuscript was sent on June 01, 2021 and accepted on August 21, 2022.

quality problem in microgrids using a co-optimization approach that combines fuzzy logic with genetic algorithms. Nonetheless, the protection coordination only considers a single type of curve which limits the solution space of the problem. In [4], the authors propose a communication-assisted dual setting relay protection scheme for microgrids. The proposed approach relies on the use of dual setting DOCRs capable of operating in both forward and reverse directions, with different settings. The problem is formulated as a non-linear constrained programming problem, in which the relay settings are optimally determined to minimize the overall relay operating time for both primary and backup operation. The main limitation of this approach is the number of optimization variables considered for each relay. Depending on the size and location of DG units within the network, these can have an impact on the protection coordination of DOCRs. In [5], the authors propose a protection coordination index (PCI) which serves as an indicator when planning the protection coordination of microgrids with high participation of DG. A two-phase non-linear programming (NLP) optimization problem is proposed to determine the PCI by optimally calculating variations in the DG penetration levels. The proposed approach does not solve the protection coordination problem, but instead, indicates the impact of connecting DG at certain locations of the system.

In [6] the coordination of DOCRs is performed considering the N-1 security criterion. In this case, the authors consider whether the system is operating in the grid-connected or islanded mode. Furthermore, the proposed approach is formulated as a mixed NLP problem including coordination constraints corresponding to the various possible outages within the microgrid. The main limitation of this approach is the limited number of decision variables considered for each relay. In [7], an adaptive protection coordination approach is proposed for DOCRs by using intelligent electronic devices and a communication channel to obtain real-time information to update the configuration of the relays. The optimal coordination is carried out through interior point optimization using AMPL. Although the proposed approach is able to handle different operating conditions of the system, including loss of loads, generations, and lines its main limitation lies on the fact of not considering different characteristic curves of the relays. The authors in [8] propose a multi-agent protection scheme for microgrids, based on a variable tripping time differential protection scheme that can operate in both grid-connected and islanded mode. The main contribution of the authors is the avoidance of nuisance tripping due to eventual DG stability problems; nonetheless, the standard features of the DOCRs are only taken into consideration, limiting the solution space of the coordination problem. In [9], the authors propose a cuckoo search optimization algorithm combined with linear programing for the optimal coordination of DOCRs in microgrids considering grid-connected and islanded modes. In this case, the authors limit the search only for the optimum value of the fault current limiter at the point of common coupling neglecting other optimization variables associated with DOCRs.

The aforementioned methodologies used to solve the optimal coordination problem in microgrids have a common denominator which is the fact of only considering standard characteristics of DOCRs. Only recently, few studies have begun to consider non-standard features of DOCRs for protection coordination in microgrids. In [10], the authors provide a well-defined analytical examination of the limitations in the tripping characteristics of manufactured DOCRs. They also proposed a new constraint regarding the *PSM* for improving the protection coordination in microgrids. In this case, the upper limit for the *PSM* was modified, expanding the tripping characteristic of DOCRs. This allows to explore a wider solution space within the coordination problem and results in faster coordination times. The authors in [11] investigate the influence of excessive fault current due to DG penetration on conventional IEC characteristics. Furthermore, a new constraint is proposed to be included in the protection coordination problem which considers the limitation of conventional IEC tripping characteristics used in numerical relays. Basically, the authors of [11] propose to set the upper limit of the *PSM* which allows changing the tripping characteristic of the relay, altering its sensitivity. Based on the works presented in [10] and [12], the authors in [12] implement the upper limit of the *PSM* as a decision variable, obtaining faster responses and guaranteeing coordination between main and back up relays.

References [10]-[12] set the bases for exploring non-standard characteristics of DOCRs in microgrids. Nonetheless, they only relate to the PSM limit and consider a single type of curve. In contrast, this paper not only considers the maximum limit of the *PSM* as a decision variable, but also takes into account different types of curves. In this case, three decision variables are optimized for each relay: namely, *TMS* the standard characteristic curve (*SCC*), and maximum limit of the *PSM*. The last two variables are considered as non-standard characteristics within the protection coordination problem since most research works consider the PSM limit as a parameter and only use a single standard curve for all relays. In this sense, the objective of this paper is to propose a novel approach of the protection coordination problem that considers non-standard characteristics of DOCRs. This allows to explore a wider solution space and therefore find better solutions to the protection coordination problem in microgrids.

II. Mathematical Modeling

The objective function of the optimal coordination problem consists on minimizing the operation time of the DOCRs as indicated in (1). In this case, t_{if} is the operation time of relay i when fault f takes place, while m and n represent the number of relays and faults, respectively.

$$min \sum_{i=1}^{m} \sum_{f=1}^{n} t_{if} \tag{1}$$

The objective function given by (1) is subject to a set of constraints as described by (2) - (8). The coordination criterion is stablished in (2). This indicates that the back up relay must actuate after the main relay with a margin of time known as *CTI* (coordination time interval). In this case, t_{if} and t_{jf} are the

operation time of main and back relays, respectively.

$$t_{if} - t_{if} \geq CTI \quad (2)$$

A general expression of the IEC and IEEE standard characteristics curves is presented in (3) (see Table 1). In this case, A, B and C are constant parameters of the relay curve, TMS_i is the time multiplying setting of relay *i*, PSM_i is the ratio between the fault current (I_{fi}) and the pickup current ($ipickup_i$) of relay *i*. One of the contributions of this paper is the fact of selecting the characteristic curve of the relay from the set of curves detailed in Table I.

$$t_{if} = \frac{A.TMS_i}{(PSM_i)^B - 1} + C \quad (3)$$

TABLE I
IEC AND IEEE STANDARD CHARACTERISTIC CURVES

Type of characteristic curve	A	B	C
Short time inverse (IEC STI)	0.05	0.04	0
Standard inverse (IEC SI)	0.14	0.02	0
Very inverse (IEC VI)	13.5	1	0
Extremely inverse (IEC EI)	80	2	0
Long time inverse (IEC LTI)	120	1	0
Moderately Inverse (IEEE MI)	0.0515	0.020	0.1140
Very inverse (IEEE VI)	19.61	2	0.4910
Extremely inverse (IEEE ME)	28.2	2	0.1217
Inverse (IEEE I)	44.6705	2.0938	0.8983
Short Inverse (IEEE SI)	1.3315	1.2969	0.16965
Long inverse (IEEE LI)	28.0715	1	10.9296

Lower and upper limits of the of PSM are represented in (4), denoted as PSM_{imin} and PSM_{imax}, respectively. In traditional OCRs coordination, these limits are fixed. However, the upper limit of the *PSM* is considered as a decision variable as indicated by (5).

$$PSM_{imin} \leq PSM_i \leq PSM_{imax} \quad (4)$$

$$\alpha \leq PSM_{imax} \quad \leq \beta \quad (5)$$

The expressions given by (6)-(8) indicate the lower and upper limits of the operation time, time setting multiplying and pickup current, respectively.

$$t_{imin} \leq t_{if} \leq t_{imax} \quad (6)$$

$$TMS_{imin} \leq TMS_i \leq TMS_{imax} \quad (7)$$

$$ipickup_{imin} \leq ipickup_i \leq ipickup_{imax} \quad (8)$$

III. SOLUTION APPROACH

The model given by (1) - (8) was solved using a GA implemented in Matlab. GAs are based on the Darwinian evolution process and have shown to be effective in dealing with complex optimization problems as reported in [12] and [13]. The flowchart of the implemented GA is depicted in Fig. 1.

A. Initial Population

The GA begins with an initial population of candidate solutions. Each candidate solution, also known as individual, is represented through an array that codifies a possible solution to the optimal coordination problem. Three optimization variables are considered for each relay: TMS, PSMimax and SCC. Therefore, the length of the vector is three times the number of relays present in the network. The initial population is randomly generated considering the limits of each decision variable. For the sake of simplicity, the relays are labeled with numbers ranging from 1 to n (n is the number of relays in the test network) preceded by the letter R. Fig. 2 shows an example of a candidate solution or individual.

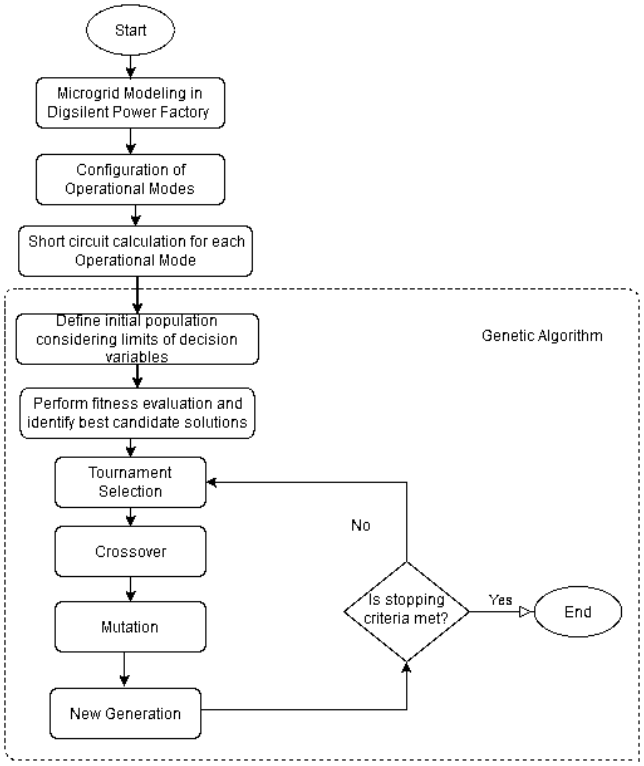

Fig 1. Flowchart of the implemented GA.

TMS R1	.....	TMS R*n*	PSM*imax* R1	.....	PSM*imax* R*n*	SCC R1	.....	SCC R*n*
0,05	.....	0,9	10	.....	40	IEC LTI	.....	IEEE I

Fig 2. Example of a candidate solution or individual

B. Fitness Evaluation

An objective function or fitness is associated to every individual of the initial population. This is done by evaluating (1) with the information encoded in every candidate solution and penalizing those who violate any constraint of the coordination problem. Fig. 3 exhibits the process of fitness evaluation.

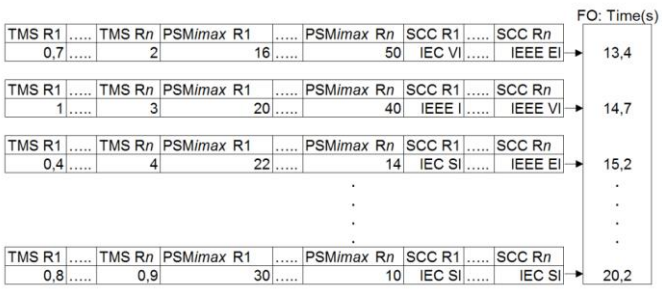

Fig. 3. Illustration of fitness evaluation

C. *Tournament Selection*

The selection stage is performed by tournament as depicted in Fig. 4. In this case, two individuals are randomly chosen from the current population and the best one (in terms of its fitness) is selected as a parent. Every two tournaments generate a couple of parents that must go through the crossover stage described in the next section. In this case, the number of tournaments carried out is equal to number of individuals.

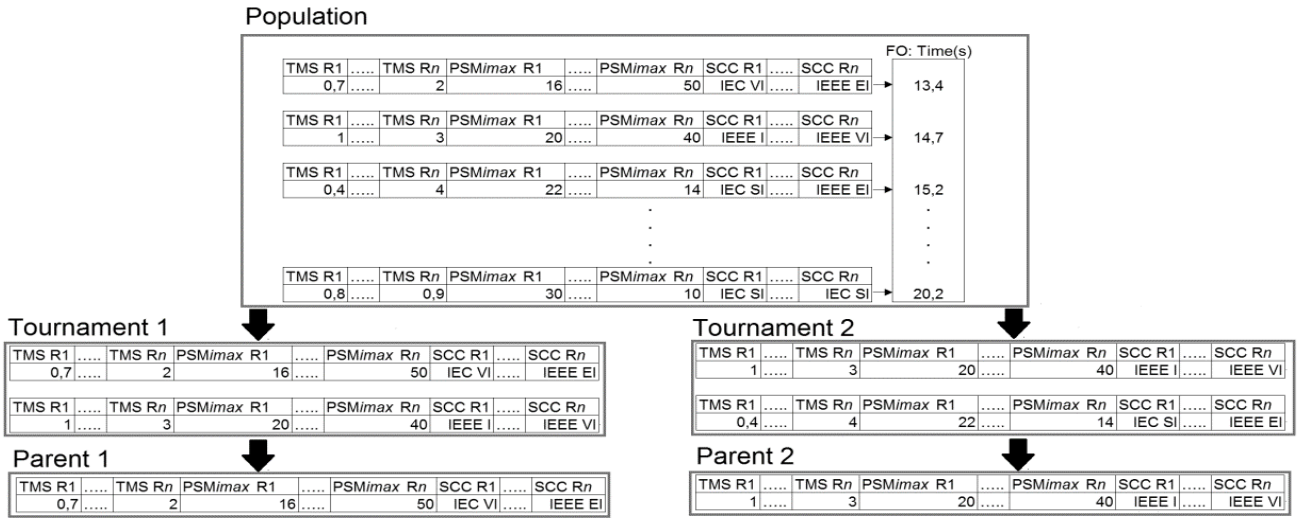

Fig 4. Tournament selection

D. *Crossover*

In this step, the parents selected in the tournament are recombined to generate two offspring. For every pair of parents, the point of recombination is randomly selected, and the new offspring share part of the information of both parents. Fig. 5 shows an example of the crossover stage for a couple of parent individuals.

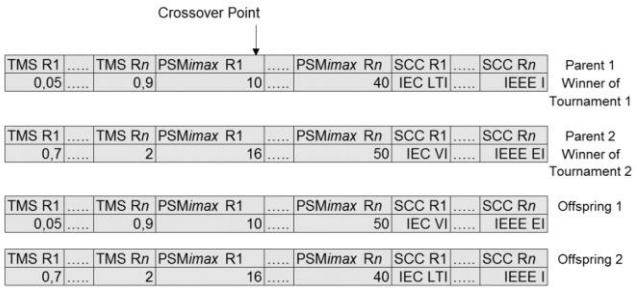

Fig 5. Crossover

E. *Mutation*

The mutation stage consists of introducing, with a given probability, small variations on the individuals resulting from the crossover. This step is designed to introduce diversification allowing the GA to eventually escape from local optimal solutions.

The changes performed in the mutation stage must guarantee that the new value of the decision variable remains within its limits. Fig. 6 exhibits an example of the mutation stage where the type of curve of a relay is changed.

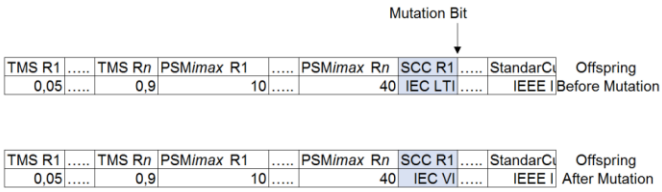

Fig 6. Example of mutation

F. *New Generation*

Right after the recombination and mutation stages, the population representing both parents and offspring is grouped together. Then the population is reduced again to its original size by discarding the worst individuals. The GA stops when a predefined number of generations is reached.

IV. Tests And Results

Several tests were carried out on a modified version of the IEEE 30-bus test system as shown in Fig. 7. The only modification carried out was only considering the distribution portion of the test system. The remain distribution system features three distribution substations at 132/33kV, and 20 feeders equipped with 29 directional OCRs labeled from R1 to R29. Furthermore, it is supposed that this system operates in grid-connected and islanded modes. Twenty faults were considered labeled from F1 to F20. For the sake of simplicity and without loss of generality, these correspond to three-phase faults that are supposed to take

place in the middle of the line. Nonetheless any other number or type of fault can also be considered. The short circuit levels of these faults are presented in Table II, which were obtained through simulation using the DigSilent Power Factory software. On the other hand, several tests were carried out to find the right tunning of the GA parameters. The number of generations, population size as well as mutation and crossover rates were tested with different values. The best performance of the GA was achieved considering 2000 generations, a population size of 200 with crossover and mutation rates of 0.7 and 0.3, respectively.

TABLE II
SHORT CIRCUIT LEVELS IN KV FOR DIFFERENT FAULTS

Fault	Grid Connected	Islanded	Fault	Grid Connected	Islanded
F1	12.97	6.03	F11	6.07	2.71
F2	3.46	2.22	F12	3.71	1.89
F3	6.31	3.76	F13	3.33	1.87
F4	9.42	5.31	F14	1.75	1.27
F5	12.25	5.76	F15	7.38	5.24
F6	6.26	5.12	F16	9.72	6.10
F7	8.36	6.13	F17	13.4	5.89
F8	13.29	9.24	F18	9.79	6.33
F9	7.14	5.17	F19	11.56	8.01
F10	11.49	5.49	F20	9.04	5.27

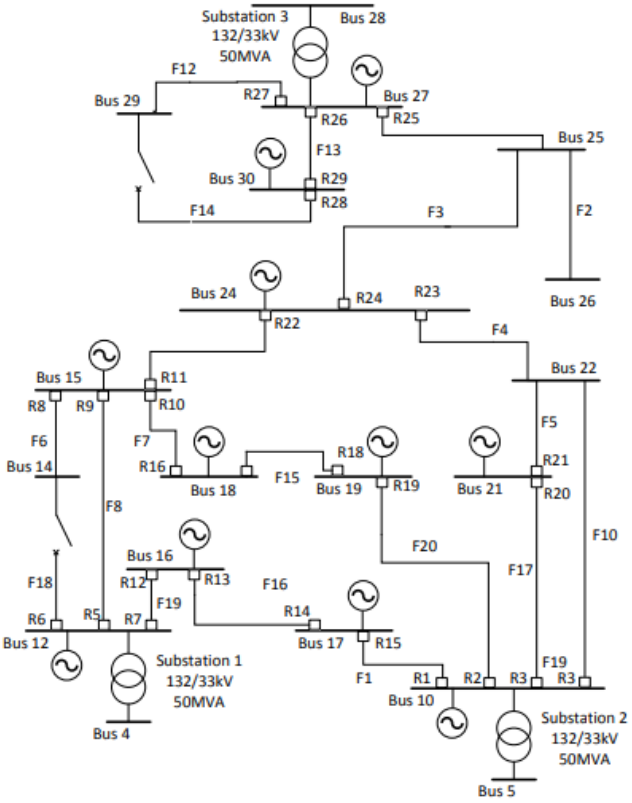

Fig 7. Microgrid under study

In the grid-connected operational mode, the load can be supplied by the DG units and the main grid. The optimization variables obtained for each relay are presented in Table III. Note that, as indicated in the formulation, three parameters are specified for each relay: *TSM*, *PSMimax* and *SCC*. Furthermore, different types of curves are used for the relays which contracts with the traditional approach where a single type of curve is use for all relays. Considering different types of curves from which to choose for each relay allows to obtain better times in the protection coordination problem. Table IV shows the operating times of main and backup relays for each fault. If the operation time is specified as NA it means that there is no fault current seen by the relay in this fault. This happens for example for backup relay 29 in faults 2, 3 and 11. In this case, the labels RP and RB indicate main and back up relays, respectively. For example, the main relay associated with fault 18 (F18) is RP5. The notation provided as RP5: 0.12 indicates that this relay operates at 0.12 seconds after this fault takes place. On the other hand, the backup relays associated with this fault are RB9 and RB13 which operate after 0.42 and 0.5 seconds respectively. In all cases, the proposed model presented admissible operating times. Also, it can be verified that the proposed approach ensures coordination between main and backup relays.

TABLE III
RELAY PARAMETERS FOR GRID-CONNECTED MODE

Relay	TSM	PSMimax	Curve	Relay	TSM	PSMimax	Curve
R1	7.59	58.71	IEC (EI)	R16	0.05	36.80	IEEE (VI)
R2	0.27	21.83	IEEE (MI)	R17	0.05	11.66	IEEE (MI)
R3	0.25	76.07	IEEE (EI)	R18	0.05	52.37	IEEE (EI)
R4	0.43	68.89	IEC (VI)	R19	0.69	49.08	IEC (EI)
R5	0.34	81.03	IEEE (MI)	R20	1.66	56.55	IEEE (EI)
R6	0.05	81.84	IEEE (EI)	R21	1.59	71.32	IEEE (EI)
R7	2.59	60.94	IEEE (EI)	R22	1.02	74.71	IEC (EI)
R8	0.29	81.83	IEEE (MI)	R23	0.38	58.26	IEEE (MI)
R9	0.08	41.11	IEEE (MI)	R24	1.37	61.59	IEC (EI)
R10	0.45	62.96	IEC (EI)	R25	0.05	89.19	IEEE (EI)
R11	0.22	84.62	IEC (SI)	R26	0.27	42.84	IEEE (SI)
R12	0.40	54.62	IEEE (EI)	R27	0.40	62.23	IEC (EI)
R13	0.15	71.92	IEEE (SI)	R28	0.12	72.81	IEC (SI)
R14	0.45	64.90	IEEE (MI)	R29	0.75	71.38	IEEE (EI)
R15	0.05	67.85	IEC (STI)				

TABLE IV
OPERATION TIME FOR GRID-CONNECTED MODE

Fault	Operating times of main and back up relays in seconds					
F1	RP1:0.15	RB23:1.4	RB21:2.2	RB20:1.6	RB19:1.2	RP15:0.52 RB13.0.2
F2	RP24:0.3	RB21:4.3	RB11:0.9	RB4:0.45	RP25:0.7	RB29: NA
F3	RP24:0.1	RB21:0.9	RB11:0.9	RB4:0.45	RP25:0.6	RB29: NA
F4	RP23:0.2	RB11:0.8 RP4:0.21	RP21:0.5 RB15:1.1	RB25:0.8 RB20:0.6	RB3:2.36 RB19:NA	
F5	RP23:0.8	RB11:1.1	RP21:0.6 RB15:0.7	RB25:1.0 RB20:2.3	RB3:0.75 RB19:1.4	RP4:0.198
F6	RP8:0.12	RB16:0.6	RB6:0.76	RB22:1.0		
F7	RP10:0.3	RB6:0.60	RB22:0.9	RP16:0.4	RB18:0.7	
F8	RP9:0.23	RB16:0.5	RB22:0.5	RP6:0.11	RB12:0.4	

F9	RP11:0.5	RB16:0.9	RB6:1.24	RP22:0.2	RB21:1.0 RB25:1.0	RB4:0.77
F10	RP23:1.0	RB11:1.3	RP21:0.8	RB25:0.7	RB20:0.7	RB19:1.6
F11	RP24:0.2	RB21:1.7	RB11:1.5	RB4:NA	RP25:0.5	RB29:NA
F12	PR27:0.1	RB24:0.6	RB29:NA			
F13	RP26:0.4	RB24:0.7	RP29:2.8			
F14	RP28:0.1	RB26:0.5				
F15	RP17:0.3	RB10:0.6	RP18:NA	RB2:NA		
F16	RP17:0.2	RB1:0.53	RP13:0.3	RB7:0.66		
F17	RP20:0.6	RB23:0.9	RP3:0.33	RB15:0.6	RB23:0.96	RB21:0.637 RB19:1.066
F18	RP5:0.12	RB9:0.42	RB13:0.5			
F19	RP12:0.2	RB14:0.5	RP7:0.14	RB9:0.49		
F20	RP19:0.5	RB17:0.8	RP2:0.27	RB15:1.1	RB23:4.22	RB21: NA

In the islanded mode, the load is only supplied by the DG units. The parameters of the relays found by the algorithm are presented in Table V. As in the previous case, it is worth noticing that different types of curves are selected, being the IEEE (EI) one of the most common ones. Table VI specifies the operation times for main and back up relays for the different faults under analysis. In this case, there are between 2 to 4 backup relays for each fault. For example, fault F18 has a main relay RP5 which operation time is 0.1328 and as backup relays RB9 and RB12 with operation times of 0.4328 and 3.81 seconds, respectively. On the other hand, fault F7 has as main relay RP10 that operates at 0.591 seconds, and 4 backup relays: RB6, RB22, RB 16 and RB18 which operate at 0.892, 0.891, 0.262 and 0.562 seconds respectively. Finally, there are some faults with two main relays such as F1, F2, F4, F9, F10, F11, F17 and F20.

TABLE V
RELAY PARAMETERS FOR ISLANDED MODE

Relay	TSM	PSMim	Curve	Relay	TSM	PSMimax	Curve
R1	0.098	87.895	IEC (EI)	R16	0.096	57.125	IEEE (EI)
R2	0.673	18.808	IEEE (VI)	R17	0.05	92.499	IEEE (MI)
R3	0.05	59.554	IEEE (VI)	R18	0.05	32.174	IEC (STI)
R4	0.445	81.721	IEC (VI)	R19	0.056	73.722	IEC (LTI)
R5	0.523	84.718	IEEE (MI)	R20	0.179	72.041	IEC (EI)
R6	0,05	58.388	IEEE (EI)	R21	0.221	83.426	IEEE (EI)
R7	0.072	65.220	IEC (LTI)	R22	1.325	55.664	IEC (EI)
R8	0,394	82.443	IEC (STI)	R23	0.170	56.413	IEEE (MI)
R9	0,114	79.155	IEC (STI)	R24	0.673	64.453	IEEE (MI)
R10	0.879	57.079	IEEE (VI)	R25	0.05	64.459	IEEE (EI)
R11	0.725	73.143	IEEE (MI)	R26	0.05	51.630	IEC (STI)
R12	0,163	84.079	IEEE (MI)	R27	0.405	80.675	IEC (EI)
R13	0.05	70.007	IEC (STI)	R28	0.416	74.217	IEEE (MI)
R14	0.141	66.578	IEC (SI)	R29	0.163	42.630	IEEE (EI)
R15	0.05	49,941	IEEE (EI)				

TABLE VI
OPERATION TIME FOR ISLANDED MODE

Fault	Operating times of main and back up relays in seconds				
F1	RP1:0.2418 RP15:1.047	RB23:1.554 RB13: 1.1379	RB21:3.66	RB20:0.774	RB19:1.33
F2	RP24:0.514 RP25:2.53	RB21:8.9 PRB29: NA	RB11:2.01	RB4:2.44	
F3	RP24:0.498	RB21:1.96	RB11:1.30	RB4:NA	RP25:1.54 RB29:NA
F4	RP23:0.593 RP4:0.1023	RB11:1.21 RB15:2.02	RP21:1.12 RB20:0.478	RB25:2.12 RB19:2.34	RB3:1.55
F5	RP23:1.17	RB11:1.49	RP21:0.910	RB25:2.66	RB3:1.21
F6	RP8:0.1259	RB16:0.481	RB6:0.9496	RB22:0.613	
F7	RP10:0.591	RB6:0.8922	RB22:0.891	RP16:0.262	RB18:0.562
F8	RP9:0.1080	RB16:0.407	RB22:0.525	RP6:0.5997	RB12:NA
F9	RP11:0.861 RB4:NA	RB16:NA RB25:3.41	RB6:1.21	RP22:0.3261	RB21:2.73
F10	RP23:1.36 RP4:0.0353	RB11:1.66 RB15:1.43	RP21:3.13 RB20:6.44	RB25:3.43 RB19:1.41	RB3:NA
F11	RP24:0.508 RB29:NA	RB21:4.46	RB11:1.74	RB4:NA	RP25:1.37
F12	RP27:0.153	RB24:0.528	RB29:NA		
F13	RP26:0.210	RB24:0.534	RP29:2.48		
F14	RP28:0.040	RB26:0.340			
F15	RP17:0.702	RB10:1.032	RP18:0.224	RB2:0.5243	
F16	RP14:0.196	RB1:0.4967	RP13:0.670	RB7:0.9704	
F17	RP3:0.9967 RP20:0.452	RB15:1.296 RB23:12966	RB23:1.2966	RB21:.2966	RB19:1.2966
F18	RP5:0.1328	RB9:0.4328	RB12:3.81		
F19	RP12:0.053	RB14:0.355	RP7:0.2619	RB9:NA	
F20	RP2:0.2705 RP19:0.9128	RB15:1.986 RB17:1.21	RB23:2.48	RB21:NA	RB20:1.4

V. CONCLUSIONS

One of the new challenges in designing protection schemes for microgrids, is to deal with their dynamic behavior resulting from the use of intermittent energy resources and their flexible configuration (connected or disconnected from the main power grid). This paper deals with this issue by proposing an adaptive protection coordination approach for optimal coordination of OCRs in microgrids that operate in different topological conditions. The main contribution of this paper is the use of non-standard features of directional over-current relays. Three optimization variables for each relay are simultaneously considered: *TMS*, *PSMimax* and *SCC*. The last two variables are not considered in traditional protection coordination approaches since the maximum limit of the *PSM* is usually considered as a constant and only a single curve is used for each relay. Including these new decision variables expands the search space of the coordination alternatives, improving the performance of the overall protection scheme. A genetic

algorithm was used to solve the proposed coordination model and several tests were performed with a microgrid that presents different operating modes. The results obtained evidenced the applicability and effectiveness of the proposed approach.

Acknowledgements
The authors gratefully acknowledge the support from the Colombia Scientific Program within the framework of the call Ecosistema Científico (Contract No. FP44842-218-2018). The authors also want to acknowledge Universidad de Antioquia for its support through the project Estrategia de Sostenibilidad.

REFERENCES

[1] B. J. Brearley and R. R. Prabu, "A review on issues and approaches for microgrid protection," Renew. Sustain. Energy Rev., vol. 67, pp. 988–997, Jan. 2017, doi: 10.1016/j.rser.2016.09.047.

[2] Y. Damchi, H. R. Mashhadi, J. Sadeh, and M. Bashir, "Optimal coordination of directional overcurrent relays in a microgrid system using a hybrid particle swarm optimization," in 2011 International Conference on Advanced Power System Automation and Protection, Oct. 2011, vol. 2, pp. 1135–1138, doi: 10.1109/APAP.2011.6180976.

[3] A. E. Dahej, S. Esmaeili, and H. Hojabri, "Co-Optimization of Protection Coordination and Power Quality in Microgrids Using Unidirectional Fault Current Limiters," IEEE Trans. Smart Grid, vol. 9, no. 5, pp. 5080–5091, Sep. 2018, doi: 10.1109/TSG.2017.2679281.

[4] H. M. Sharaf, H. H. Zeineldin, and E. El-Saadany, "Protection Coordination for Microgrids With Grid-Connected and Islanded Capabilities Using Communication Assisted Dual Setting Directional Overcurrent Relays," IEEE Trans. Smart Grid, vol. 9, no. 1, pp. 143–151, Jan. 2018, doi: 10.1109/TSG.2016.2546961.

[5] H. H. Zeineldin, Y. A.-R. I. Mohamed, V. Khadkikar, and V. R. Pandi, "A Protection Coordination Index for Evaluating Distributed Generation Impacts on Protection for Meshed Distribution Systems," IEEE Trans. Smart Grid, vol. 4, no. 3, pp. 1523–1532, Sep. 2013, doi: 10.1109/TSG.2013.2263745.

[6] K. A. Saleh, H. H. Zeineldin, and E. F. El-Saadany, "Optimal Protection Coordination for Microgrids Considering N-1 Contingency," IEEE Trans. Ind. Inform., vol. 13, no. 5, pp. 2270–2278, Oct. 2017, doi: 10.1109/TII.2017.2682101.

[7] M. N. Alam, "Adaptive Protection Coordination Scheme Using Numerical Directional Overcurrent Relays," IEEE Trans. Ind. Inform., vol. 15, no. 1, pp. 64–73, Jan. 2019, doi: 10.1109/TII.2018.2834474.

[8] T. S. Aghdam, H. K. Karegar, and H. H. Zeineldin, "Variable Tripping Time Differential Protection for Microgrids Considering DG Stability," IEEE Trans. Smart Grid, vol. 10, no. 3, pp. 2407–2415, May 2019, doi: 10.1109/TSG.2018.2797367.

[9] E. Dehghanpour, H. K. Karegar, R. Kheirollahi, and T. Soleymani, "Optimal Coordination of Directional Overcurrent Relays in Microgrids by Using Cuckoo-Linear Optimization Algorithm and Fault Current Limiter," IEEE Trans. Smart Grid, vol. 9, no. 2, pp. 1365–1375, Mar. 2018, doi: 10.1109/TSG.2016.2587725.

[10] S. M. Saad, N. El-Naily, and F. A. Mohamed, "A new constraint considering maximum PSM of industrial over-current relays to enhance the performance of the optimization techniques for microgrid protection schemes," Sustain. Cities Soc., vol. 44, pp. 445–457, Jan. 2019, doi: 10.1016/j.scs.2018.09.030.

[11] N. Elnaily, S. Saad, T. Elmenfy, and F. Mohamed, "A Novel Constraint and Non-Standard Characteristics for Optimal Overcurrent Relays Coordination to Enhance Microgrid Protection Scheme," IET Gener. Transm. Distrib., vol. 13, 2019, doi: 10.1049/iet-gtd.2018.5021.

[12] S. D. Saldarriaga-Zuluaga, J. M. López-Lezama, and N. Muñoz-Galeano, "Optimal Coordination of Overcurrent Relays in Microgrids Considering a Non-Standard Characteristic," Energies, vol. 13, no. 4, Art. no. 4, Jan. 2020, doi: 10.3390/en13040922.

[13] L. Agudelo, J. M. López-Lezama, and N. Muñoz, "Análisis de Vulnerabilidad de Sistemas de Potencia Mediante Programación Binivel," Inf. Tecnológica, vol. 25, no. 3, pp. 103–114, 2014, doi: 10.4067/S0718-07642014000300013.

[14] University of Illinois. ICSEG Power Case 1 - IEEE 30 bus test system. Available online https://uofi.app.box.com/s/frjqsg9vpe6dvv7ufodd (accessed in July 2021).

Sergio Danilo Saldarriaga Zuluaga, Facultad de Ingeniería, Institución Universitaria Pascual Bravo, Calle 73 No 73A-226, Medellín, Colombia. He received his B.Sc. and M.Sc. degrees from the Universidad de Antioquia in 2013 and 2016, respectively. He is currently working towards the Ph.D. degree in electronic and computing engineering at the Universidad de Antioquia. Currently he is a Professor at Institución Universitaria Pascual Bravo, Medellín, Colombia. His major research interests are planning, operation and protection of electrical power systems.
ORCID: https://orcid.org/0000-0002-9134-8576.

Jesús M. López Lezama, Departamento de Ingeniería Eléctrica, Facultad de Ingeniería, Universidad de Antioquia, Calle 70 No 52-21, Medellín Colombia. He received his B.Sc. and M.Sc. degrees from the Universidad Nacional de Colombia in 2001 and 2006, respectively. He also received his Ph.D. degree at the Universidade Estadual Paulista (UNESP), SP, Brazil in 2011. Currently he is an associate Professor at Universidad de Antioquia, Medellín, Colombia. His major research interests are planning and operation of electrical power systems and distributed generation.
ORCID: https://orcid.org/0000-0001-6213-4133

Nicolás Muñoz-Galeano, Departamento de Ingeniería Eléctrica, Facultad de Ingeniería, Universidad de Antioquia, Calle 70 No 52-21, Medellín Colombia. He received a B. E. degree in Electric Engineering at the University of Antioquia (UdeA-2004), and the Ph.D. degree in Electronics Engineering (UPVLC-2011). Since 2005 he has been professor of the Electric Engineering Department at the University of Antioquia (Colombia) and member of research group GIMEL. His research work is focused in power electronics design, control and electrical machines.
ORCID: https://orcid.org/0000-0003-1407-5559